SHORT-PERIOD SEISMIC WAVES GENERATED IN ASPERITY MODELS BY DYNAMIC SIMULATION OF FAULT RUPTURING

Dan Kazuo[1] and Okazaki Atsushi[2]

[1] *Institute of Technology, Shimizu Corporation, 4-17, Etcyujima 3-Chome, Koto-Ku, Tokyo 135-8530, Japan*
[2] *The Kansai Electric Power Company, 6-16, Nakanoshima 3-Chome, Kita-Ku, Osaka 530-8270, Japan*
Email: kazuo.dan@shimz.co.jp, okazaaki.atsushi@e3.kepco.co.jp

ABSTRACT:

In Japan, asperity models, consisting of asperities of high stress drop and backgrounds of no stress drop, are often adopted as kinematic source models for predicting strong ground motions from scenario earthquakes. The asperities are assumed to generate long-period seismic motions more and short-period seismic motions far more than the backgrounds.
In order to specify the asperity models, two theoretical equations and one empirical equation are applied to evaluation of the three parameters out of the following six parameters: the area of the entire fault, the seismic moment, the averaged stress drop, the area of the asperity, the stress drop of the asperity, and the amplitude of the acceleration source spectrum in the short-period range.
Since the empirical equation describing that the amplitude of the acceleration source spectrum in the short-period range is proportional to the product of the stress drop on the asperity and the size of the asperity had not been studied systematically, we carried out the dynamic simulation of fault rupturing of the asperity models to verify this empirical equation. The faults were assumed to be 15 km long and 10 km wide with the asperity of 5.8 km by 5.8 km located in various positions, and the dynamic simulation was carried out by the three dimensional finite difference method.
Most of the results showed that the asperities generated the short-period seismic waves more than the backgrounds did as granted in the current researches. But, some of the results showed that the backgrounds generated the short-period seismic waves as much as the asperities did. All of the results showed that the peak of the velocity slip time-function increased on the fault far from the hypocenter, because more strain energy released on the ruptured area could be applied to the fracture energy on the fault far from the hypocenter. This phenomenon indicated that we should check the location of the area that generates the short-period seismic waves based on the relative location of the hypocenter, when we specify the asperity models for predicting the strong ground motions from scenario earthquakes.

KEYWORDS: Strong motion prediction, asperity model, short-period level, dynamic simulation

1. INTRODUCTION

The asperity models are often adopted in Japan for predicting the strong ground motions from the scenario earthquakes, which were originally proposed as characterized source models by Somerville *et al*. (1993).
The fault parameters are specified based on the physical features of the asperity model (Headquarters for Earthquake Research Promotion, 2005). The physical features are the following two theoretical equations and one empirical equation among the six major parameters of the area of the entire fault S, the seismic moment M_0, the averaged stress drop $\Delta\sigma$, the area of the asperity S_{asp}, the stress drop of the asperity $\Delta\sigma_{asp}$, and the amplitude of the acceleration source spectrum in the short-period range A (short-period level, hereafter):

$$\Delta\sigma = (7/16)\,[M_0/(S/\pi)^{3/2}], \tag{1.1}$$

$$\Delta\sigma_{asp} = (S/S_{asp})\Delta\sigma, \tag{1.2}$$

$$A = 4\pi (S_{asp}/\pi)^{1/2} \Delta\sigma_{asp} \beta^2, \quad (1.3)$$

Here, β is the *S*-wave velocity of the medium at the source. Equation (1.1) is a theoretical equation among the averaged stress drop, the seismic moment, and the fault area of a circular crack model derived by Eshelby (1957), equation (1.2) is a general equation for asperity models derived by Madariaga (1979), and equation (1.3) comes from an empirical equation proposed by Brune (1970) for circular crack models.
Dalguer *et al*. (2004) examined equation (1.1) for the asperity models with the fault parameters varying systematically. Dan *et al*. (2002) proved that equation (1.2) can be applied together with equation (1.1) to the asperity models in which the asperities are located randomly on the fault.
Madariaga (1977) studied the dynamic rupturing of the fault, and showed the short-period level generated in circular crack models was compatible to Brune's empirical equation. Boatwright (1988) showed that the asperity model generated the similar short-period level as the circular crack model when the radius and the stress drop of the asperity were the same as those of the circular crack. But no systematical examinations have been performed so far.
Hence, we examined whether the short-period level could be estimated by equation (1.3) through the dynamic rupture simulation of several asperity models with the fault parameters varying systematically.
Two out of those results are shown and explained in the following sections.

2. MODELS

Figure 1(a) shows the asperity model examined for the first step. The dip angle was 90 degrees (vertical fault), and the rake was 0 degrees (lateral slip). The fault length was 15 km, and the fault width was 10 km from 5 to 15 km deep. The area of the asperity was assumed to be 5.8 km×5.8 km, 22 % of the entire fault based on the statistics obtained by Somerville *et al.* (1999). The asperity was located in the shallower part of the fault. The rupture initiation area was assumed to be located in the deepest part of the asperity. The *P*-wave velocity was 6 km/s, the *S*–wave velocity was 3.464 km/s (Poisson solid assumption), and the density was 2.7 g/cm^3. We changed the location of the asperity systematically. Figure 1(b) shows one of the models, in which the asperity is located in the center of the fault deeper than the asperity in Figure 1(a).
We applied the finite difference method developed by Pitarka *et al*. (2005) to the dynamic rupture simulation of the faults. The media were assumed to be elastic, and the media were connected on the fault by the slip weakening models (Ohnaka and Matsu'ura, 2002). Figure 2 shows the slip weakening models on the fault adopted in this study. Here, D_c is the slip weakening distance, *SE* is the strength excess, and $\Delta\sigma_d$ is the dynamic stress drop. We assumed the common D_c for the rupture initiation area, the asperity, and the background and the common breakdown stress drop $\Delta\sigma_b$ ($SE+\Delta\sigma_d$) for the rupture initiation area and the asperity.
The mesh size was 0.05 km, and then the effective period was over 0.12 seconds when one wave length was described in 8 meshes.

3. RESULTS

Figure 3 shows the results of the dynamic rupture simulation of the asperity model in Figure 1(a).
Figure 3(a) shows the final slips on the fault, indicating the peak of 1.2 m. We calculated the seismic moment M_0 to be 1.7×10^{18} N·m from the final slips by the following integration:

$$M_0 = \mu \int_S D dS \approx \mu \sum_i D_i \Delta S_i. \quad (3.1)$$

Here, μ is the rigidity, *D* is the final slip, *S* is the fault plane, and *i* is the number of the meshes on the fault.
Figure 3(b) shows the slip velocity time-functions and the contour of the peak velocities. Higher peak velocities are found on the shallower part of the asperity. This is because the slip velocity was accelerated as the rupture front propagated on the asperity.

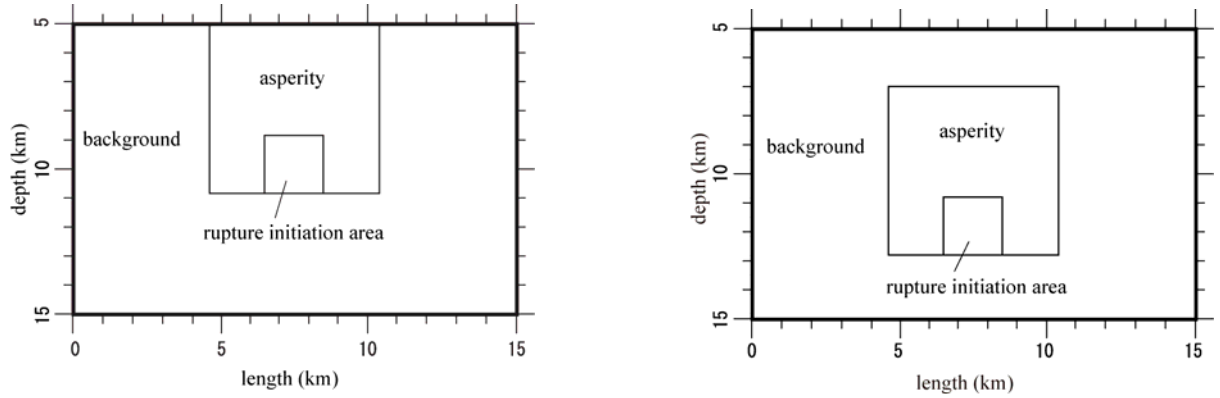

(a) shallower asperity (b) deeper asperity

Figure 1. Asperity models examined in this study.

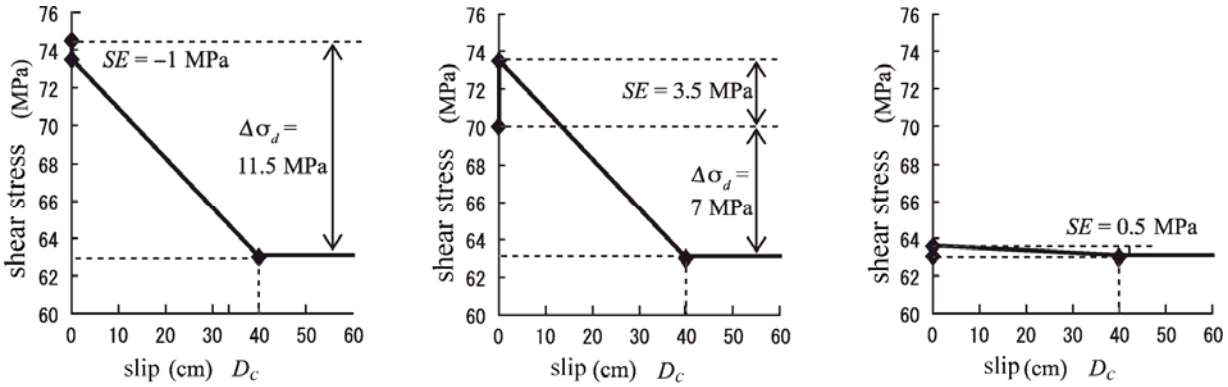

(a) rupture initiation area (b) asperity (c) background

Figure 2. Slip weakening models on the fault adopted in the asperity models.

Figure 3(c) shows the rupture time, which is defined as the time when each slip velocity time-function changes from zero to non-zero. We read the rupture propagating velocity v of 1.6 km/s in the rupture mode 2 and 1.8 km/s in the rupture mode 3 from the rupture time shown in Figure 3(c).
We calculated the source time-function from the slip velocity time-functions by

$$\Omega(t) = \mu \int_S V(\xi,t)dS \approx \mu \sum_i V_i(t)\Delta S_i. \tag{3.2}$$

Here, $V(\xi, t)$ is the slip velocity time-function at ξ on the fault.
Figure 3(d) shows the source time-functions; the thick line is for the entire fault, the chained line for the rupture initiation area, the thin line for the asperity, and the dotted line for the background. Then, we obtained the acceleration source spectrum by

$$A(\omega) = \omega^2 |\Omega(\omega)| = \omega^2 \left| \int_0^\infty \Omega(t) \exp[-j\omega t] dt \right|. \tag{3.3}$$

Here, j is the imaginary unit.
Figure 3(e) shows the acceleration source spectrum for the entire fault. We observed large high frequency amplitude beyond about 5 Hz. This high frequency amplitude comes from the rupture initiation area, because the source time-function starts abruptly at the time of zero shown in Figure 3(d).

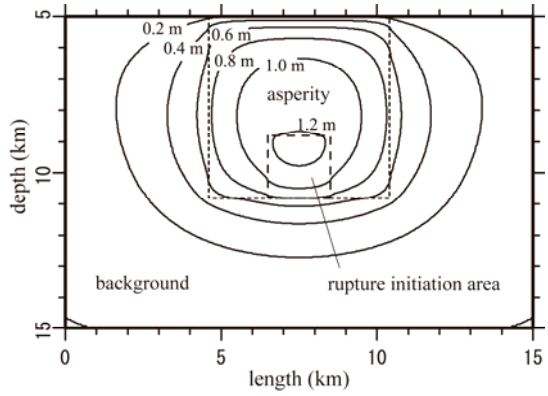

(a) final slips on the fall

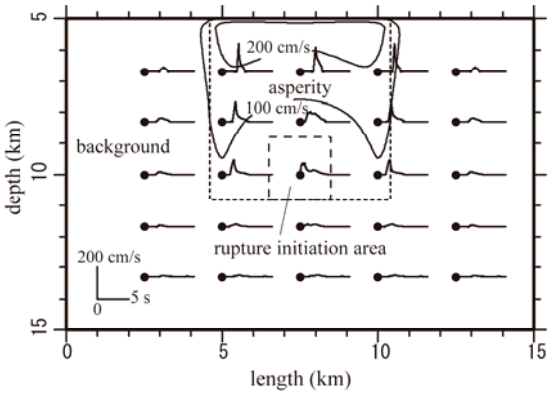

(b) slip velocity time-functions and contour of peak velocities

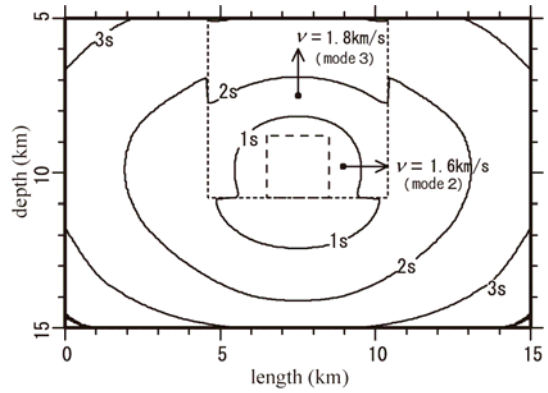

(c) rupture time

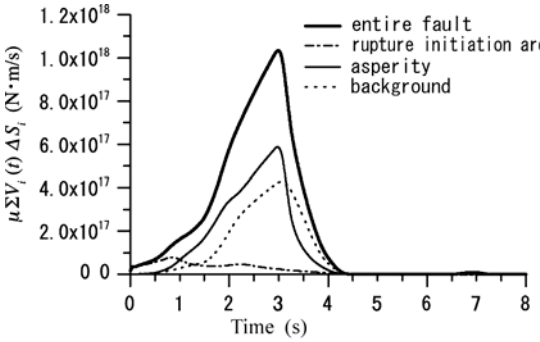

(d) source time-functions

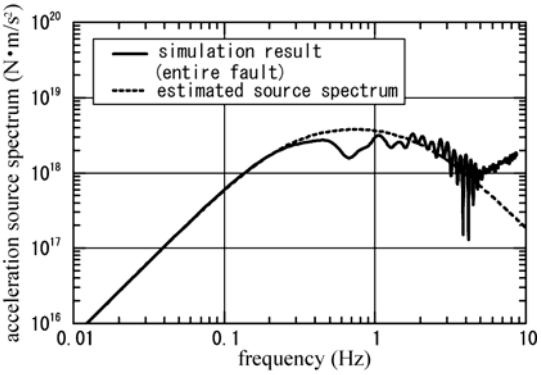

(e) acceleration source spectrum

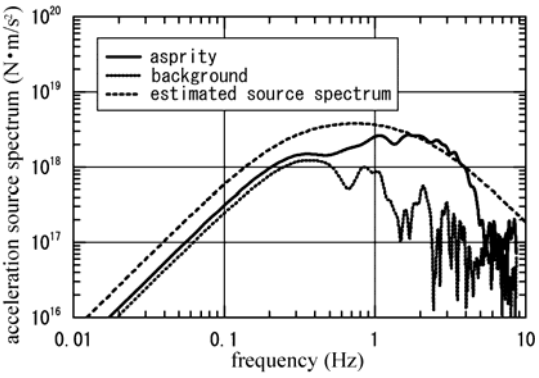

(f) acceleration source spectra of each area

Figure 3. Results of the dynamic rupture simulation of the asperity model in Figure 1(a).

On the other hand, we estimated the short-period level A to be 4.9×10^{18} N·m/s^2 by equations (1.1) to (1.3) based on the fault area of 150 km^2, the asperity area of 33 km^2, and the seismic moment of 1.7×10^{18} N·m.
The f_{max} was also evaluated by the following equation of Ohnaka and Matsu'ura (2002):

$$f_{max} = [1.9/\pi^2][v/C(v)][\Delta\sigma_b/\mu]/D_c. \quad (3.4)$$

Here, v is the rupture propagating velocity, $C(v)$ is the function of the rupture propagating velocity for each rupture mode of 2 or 3, $\Delta\sigma_b$ is the breakdown stress drop ($SE+\Delta\sigma_d$ in Figure 2), and D_c is the slip weakening distance.

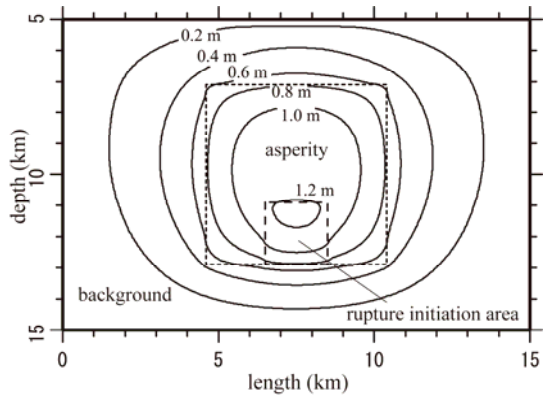

(a) final slips on the fault

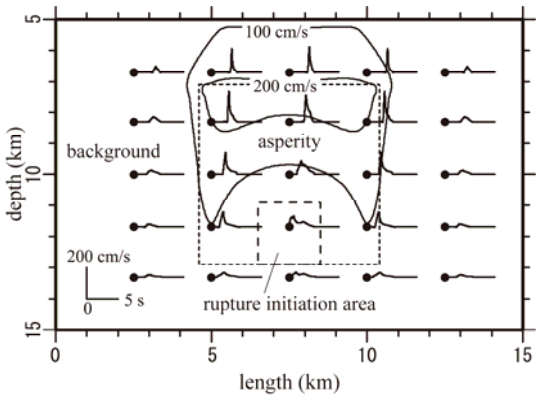

(b) slip velocity time-functions and contour of peak velocities

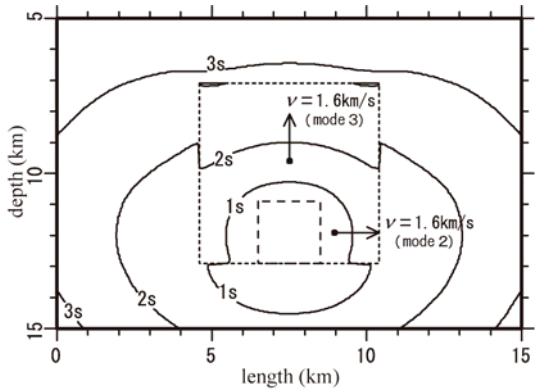

(c) rupture time

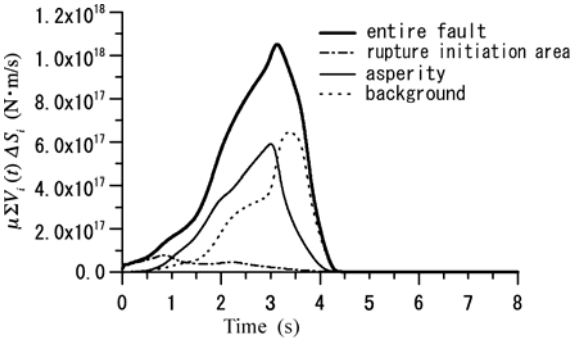

(d) source time-functions

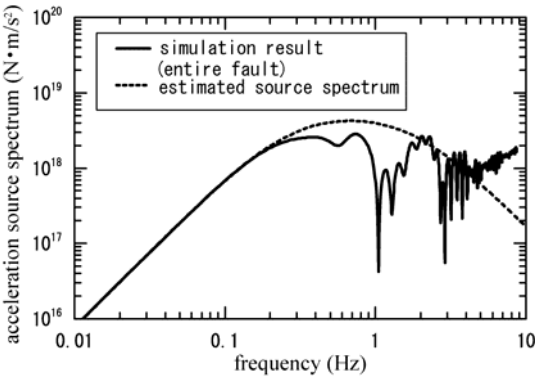

(e) acceleration source spectrum

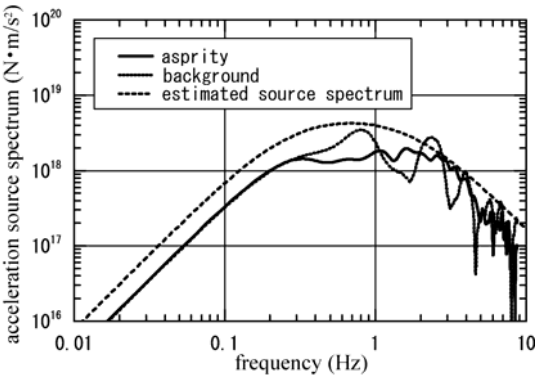

(f) acceleration source spectra of each area

Figure 4. Results of the dynamic rupture simulation of the asperity model in Figure 1(b).

Figure 3(e) shows the acceleration source spectrum estimated from the seismic moment, the short-period level, and the f_{max}. The estimated short-period level agrees well with that of the results of the dynamic rupture simulation.

On the other hand, Figure 3(f) shows the acceleration source spectra for the asperity and the background. The spectrum for the background has almost the same value as that for the asperity in the low frequency range, and even smaller value in the high frequency range. This figure indicates that the existing assumption (Headquarters for Earthquake Research Promotion, 2005) is correct that the asperity is the locked region on the fault before the earthquake, releases the cumulative stress abruptly after the locked region ruptures, has large stress drop, and causes not only large slip proportional to long-period waves but also large slip velocity proportional to short-period waves.

4. EFFECTS OF ASPERITY DEPTH TO THE SHORT-PERIOD LEVEL

Figure 4 shows another example of the results for the model in Figure 1(b). Figure 4(b) indicates that large peak velocities are generated on the background just above the asperity. This is because the slipping on this background was induced by the high speed slipping on the shallower part of the asperity.
Figure 4(e) shows that the short-period level estimated by equation (1.3) agrees well again with that of the results of the dynamic rupture simulation. But, Figure 4(f) shows that the acceleration source spectrum for the background has almost the same value as that for the asperity in the entire frequency range. This case indicates that existing assumption is not correct.
Our results correspond to the summary of Hartzell *et al*. (1996) that it is too simplistic to conclude that high frequencies originate only from low-slip regions, or conversely, only from low-frequency asperities. But, we can check the location of the area that generates the short-period seismic waves based on the relative location of the hypocenter, when we specify the asperity models for predicting the strong ground motions from scenario earthquakes.

5. ACKNOWLEDGMENTS

All the results in this paper were obtained in the research project by the group of Tokyo Electric Power Company and other 10 Japanese electric power companies.

REFERENCES

Boatwright, J. (1988): The seismic radiation from composite models of faulting. *Bulletin of the Seismological Society of America*, **78:2**, 489-508.
Brune, J.N. (1970): Tectonic stress and the spectra of seismic shear waves from earthquakes. *Journal of Geophysical Research*, **75:26**, 4997-5009.
Dalguer, L., Miyake, H. and Irikura, K. (2004): Characterization of dynamic asperity source models for simulating strong ground motion. *13th World Conference on Earthquake Engineering*, 3286.
Dan, K., Sato, S. and Irikura, K. (2002): Characterizing source model for strong motion prediction based on asperity model. *Proceedings of 11th Japan Earthquake Engineering Symposium*, 555-560 (in Japanese).
Eshelby, J.D. (1957): The determination of the elastic field of an ellipsoidal inclusion, and related problems. *Proceedings of the Royal Society of London*, **A: 241**, 376-396.
Hartzell, S., Liu, P. and Mendoza, M. (1996): The 1994 Northridge, California, earthquake: Investigation of rupture velocity, risetime, and high-frequency radiation. *Journal of Geophysical Research*, **101:B9**, 20,091-20, 108.
Headquarters for Earthquake Research Promotion (2005): *National Seismic Hazard Maps for Japan*, **2** (in Japanese).
Madariaga, R. (1977): High-frequency radiation from crack (stress drop) models of earthquake faulting. *Geophysical Journal of the Royal Astronomical Society*, **51:3**, 625-651.
Madariaga, R. (1979): On the relation between seismic moment and stress drop in the presence of stress and strength heterogeneity. *Journal of Geophysical Research*, **84:B5**, 2243-2250.
Ohnaka, M. and Matsu'ura, M. (2002): *The Physics of Earthquake Generation*. University of Tokyo Press (in Japanese).
Pitarka, A., Day, S. and Dalguer, L.A. (2005): Investigation of difference in ground motion between surface and subsurface faulting based on dynamic rupture modeling. *AGU Chapman Conference on Radiated Energy and the Physics of Earthquake Faulting*, Portland, Maine, Abstracts.
Somerville, P., Irikura, K., Sawada, S., Iwasaki, Y., Tai, M. and Fushimi, M. (1993): A study on empirical modeling of slip distribution on faults. *Proceedings of 22nd JSCE Earthquake Engineering Symposium*, 291-294 (in Japanese).